J Mater Sci (2007) 42:3299–3306
DOI 10.1007/s10853-006-0777-1

SIZE-DEPENDENT EFFECTS

Oxidation of gold metal particles supported on TiO_2: an FTIR study by means of low-temperature CO adsorption

Hr. Klimev · K. Fajerwerg · K. Chakarova · L. Delannoy · C. Louis · K. Hadjiivanov

Received: 23 May 2006 / Accepted: 8 August 2006 / Published online: 22 March 2007

Abstract Two Au/TiO_2 samples with different gold loadings (0.7 and 4.0 wt.% Au) were prepared by deposition-precipitation with urea and calcined at 673 K. TEM revealed gold particles of 3.2 and 3.9 nm for the 0.7 and 4.0 wt.% samples, respectively. The samples were subjected to different red-ox treatments and then the state of gold was determined by the FTIR spectra of CO adsorbed at low temperature. Several kinds of gold carbonyl species were detected during the experiments: (i) Au^0–CO at around 2107 cm^{-1}; (ii) Au^+–CO at ca. 2175 cm^{-1}; (iii) $Au^{\delta+}$–CO in the region of 2140–2137 cm^{-1} and (iv) $Au^{\delta'+}$–CO ($\delta' > \delta$) at around 2155 cm^{-1}. The 4.0 wt.% sample contained mainly metallic gold after evacuation at 673 K. Subsequent interaction with oxygen at 373 K leads to oxidation of a fraction of the surface metallic gold sites to $Au^{\delta+}$ sites. These sites were considered as cations located on the surface of the metal particles with a partially positive charge $\delta+$ ($0 < \delta < 1$) because of electron transfer from the gold bulk. Evacuation at 673 K leads to back reduction of the $Au^{\delta+}$ sites to metallic gold. The oxidation of gold particles was more efficient when performed with a NO + O_2 mixture. It resulted in creation of $Au^{\delta'+}$ sites with a higher positive charge than that of the $Au^{\delta+}$ sites. In this case the oxidation involved a higher number of Au^0 sites. A similar treatment of the 0.7 wt.% Au sample, however, resulted in formation of "isolated" Au^+ species. The results indicate that small metal particles are more easily oxidized by a NO + O_2 mixture. A model of the formation of the different sites, explaining well the experimental results, is proposed.

Introduction

Although the number of works devoted to the characterization of supported gold catalysts continuously increases, there is still an ongoing debate on some basic questions, such as the oxidation state of the gold sites participating in the CO oxidation reaction. Many authors support the idea that it is the metallic gold that is catalytically active [1–3]. However, a series of recent results indicate that either gold cations are the reaction active sites or their activity is superiour to that of metallic gold [4–6]. That is why determination of the oxidation state of gold in supported catalysts is of great importance.

One of the most used techniques for surface characterization is IR spectroscopy of probe molecules [7–9]. In the case of supported gold catalysts the most used probe molecule is CO [4–6, 10–31]. However, there is also disagreement in the interpretation of the IR carbonyl bands. In what follows we shall try to summarise the current state of the art of CO adsorption on gold-containing samples.

All authors are unanimous that metallic gold can be monitored by carbonyl bands between 2130 and 2100 cm^{-1} [6, 10–19, 22, 25, 26, 28–33], but in some cases at lower frequencies [20, 21]. This blue shift with

Hr. Klimev · K. Chakarova · K. Hadjiivanov (✉)
Institute of General and Inorganic Chemistry, Bulgarian Academy of Sciences, Sofia 1113, Bulgaria
e-mail: kih@svr.igic.bas.bg

K. Fajerwerg · L. Delannoy · C. Louis
Laboratoire de Réactivité de Surface, Université P. et M. Curie, 75252 Paris Cedex 05, France

respect to gaseous CO (2143 cm^{-1}) arises from the fact that CO forms mainly a weak π-back bond with gold. It is well documented that Au^0–CO bands are strongly coverage dependent [3, 10–17]. However, the shift to lower frequencies occurring when the coverage increases is the opposite of what is usually observed for CO adsorbed on other metals. Boccuzzi et al. [13] have demonstrated that this shift is due to static interaction between the CO molecules adsorbed on metallic gold sites and those adsorbed on the cations from the support. Another important observation, that will be used further on in the discussion, is that not all surface gold atoms are able to adsorb CO; it is believed that CO is only bonded to low-coordinated (defect) metal sites [11, 15, 18, 19, 22].

It is also generally accepted that the carbonyl stretching frequency of the Au$^+$–CO species is higher than that of the metallic gold carbonyls. In principle CO is bonded to Au$^+$ cations via σ and π-bonds. As a result of this and because of the synergism between the two bonds, the metal-carbon bond is stronger than is the case of Au^0–CO [5, 10, 22–24]. Most authors report that Au$^+$–CO species absorb around 2175–2160 cm^{-1} when the Au$^+$ ions are located on oxides (the so-called isolated Au$^+$ ions) [6, 15–17, 19, 21, 25] and at somewhat higher frequencies, around 2192–2176 cm^{-1}, when these cations are in zeolites [24, 26, 33]. However, lower frequencies have also been reported [23].

Many authors have reported carbonyl bands in the 2154–2116 cm^{-1} region and have assigned them to Au$^{\delta+}$–CO species [13–16, 20, 24, 27]. It is interesting to note that the wavenumbers and the stabilities of these carbonyls are intermediate between those of CO adsorbed on metallic gold and on Au$^+$ cations. As early as in 1969, Yates [25] observed, in his pioneering study, that addition of oxygen to carbonyls formed on supported metallic gold led to formation of a band at 2138 cm^{-1} and assigned it to O–Au^0–CO species. In a study of a Au/HY sample, Guillemot et al. [14] have assigned bands around 2140 cm^{-1} to carbonyls on positively charged gold clusters, Au$_n^{\sigma+}$, inside the zeolite channels. In a similar way, bands around this frequency have been attributed to carbonyls on: two-dimensional clusters positively charged because of the contact with the support [29], oxidized sites on the surface of the metal particles [17] or at their perimeter [15, 28], sites from the surface of metal particles made positive as a result of oxygen adsorption [11], positively polarized gold sites [3, 27], electron deficient metal sites [21] as well as to O$_2^{\delta-}$Au$^{\delta+}$–CO, O$^{\delta-}$Au$^{\delta+}$–CO [12] or O$_2^{-}$Au$^{\delta+}$–CO species [22].

The other stable oxidation state of gold is Au^{3+}. Bands due to surface Au^{3+}–CO species have been proposed in a very wide spectral region, namely 2274–2139 cm^{-1} [5, 22, 23, 26, 30, 31]. In most cases the assignments are tentative and ambiguous. We have already noted [16, 30] that the formation of Au^{3+}–CO surface species is unusual, because Au^{3+} cations on the as-prepared samples are coordinatively saturated and evacuation at elevated temperatures, aimed at creating c.u.s. Au^{3+} cations, leads, as a rule, to their reduction. It should also be noted that cationic gold sites are easily reduced in the presence of CO even at ambient temperature.

In a previous work on CO adsorption on 0.7 wt.% Au/TiO$_2$ [16] we reported that isolated Au$^+$ sites formed carbonyls absorbing around 2175 cm^{-1}, and Au^0–CO species were found at 2130–2100 cm^{-1}. However, detailed analysis of the bands at 2140–2130 cm^{-1} was hindered, because of the superimposition with a band at 2127 cm^{-1} due to Ti^{4+}–^{13}CO species formed with the support and ^{13}CO arising from the ^{13}C natural abundance.

The aim of this work is to study, by means of IR spectroscopy of adsorbed CO, the possibility of oxidation of metallic gold nanoparticles, paying special attention to the nature of the Au$^{\delta+}$ sites. For this purpose we studied mainly a sample with a relatively high gold concentration, namely 4 wt.%. This ensured a high relative intensity of the gold carbonyl bands and, in particular, allowed us to follow precisely the behaviour of the bands around 2140–2130 cm^{-1}. In order to obtain information on whether and how the particle size affected the oxidation of gold, we also studied another sample, containing 0.7 wt.% Au, and characterized by smaller gold particles.

Experimental

Preparation of the samples

Two Au/TiO$_2$ samples were prepared by a deposition–precipitation procedure as described elsewhere [34, 35]. Typically, a solution of HAuCl$_4$ (concentration depending on the desired gold loading) was prepared by dissolving the appropriate amount of HAuCl$_4$.3H$_2$O in 100 mL of deionized water. Urea was added to the gold solution to achieve a concentration 100 times higher than the HAuCl$_4$ concentration. The support (1 g) was then added to the solution and the suspension was heated to 353 K and stirred for 16 h in a reactor closed and kept away from light. Then, the solid was separated by centrifugation, washed three times with deionized water (with centrifugation between the washing procedures) and dried under vacuum at ambient temperature. Then the samples were calcined at 673 K for 2 h (100 mL min^{-1}, 2 K min^{-1} from ambient temperature to 673 K). The gold loading in the samples thus prepared was 0.7 and 4 wt.%, respectively.

Characterization techniques

Chemical analysis was performed by inductively coupled plasma atom emission spectroscopy at the CNRS Center of Chemical analysis (Vernaison, France).

TEM analysis was performed using a PHILIPS CM 120 (120 kV) microscope. The histograms of the metal particle sizes were established from the measurement of 300 to 1000 particles. The average gold particle diameter d_s was calculated using the following formula: $d_s = \Sigma n_i d_i^3 / \Sigma n_i d_i^2$ where n_i is the number of particles of diameter d_i. The size limit for the detection of gold particles on these supports is about 1 nm with a resolution of ±0.35 nm.

The IR spectra were recorded on a Nicolet Avatar 360 spectrometer at a spectral resolution of 2 cm^{-1} and accumulation of 64 scans. Self-supported pellets (ca. 10–20 mg cm^{-2}) were prepared from the dried sample powders and treated directly in a purpose-made IR cell which allowed measurements in the temperature interval between 100 and 293 K. The cell was connected to a vacuum-adsorption apparatus with a residual pressure below 10^{-3} Pa.

Carbon monoxide (>99.997) was supplied by Linde AG. Nitrogen monoxide (>99.0) was purchased from Messer Greisheim GmbH. Before use, carbon monoxide and oxygen were passed through a liquid nitrogen trap while NO was additionally purified by fraction distillation.

Results

Initial characterization of the samples

The TEM photographs of the two samples calcined at 673 K clearly show the presence of small metal gold particles with a rather uniform dispersion (Fig. 1), consistent with reduction of gold during the calcination as reported by many authors [10–13, 22].

With the 0.7 wt.% Au sample the gold particles are well separated from one another whereas for the 4 wt.% Au sample the metallic particles are more "gathered" on the support (Fig. 1b). The particle size distribution for the 4 wt.% Au/TiO_2 sample (Fig. 1b) is slightly broader and shifted towards larger sizes as compared to the 0.7 wt.% Au/TiO_2 sample. Calculations show that the mean particle sizes are 3.2 and 3.9 nm for the 0.7 and 4 wt.% samples, respectively.

Low-temperature CO adsorption on 4 wt.% Au/TiO_2 evacuated at 673 K

Prior to the IR experiments, the sample was activated in situ by 1 h heating in oxygen (13.3 kPa) at 673 K, followed by 1 h evacuation at the same temperature. In order to avoid the reduction of eventual cationic gold sites by CO, the adsorption experiments were performed at low temperature. Introduction of CO (400 Pa equilibrium pressure, followed by evacuation) to the sample at 100 K leads to the appearance of a very strong band at 2179 cm^{-1} and a series of bands with a weaker intensity at 2208, 2166 (shoulder), 2127 and 2107 cm^{-1} (Fig. 2, spectrum a). According to literature data [36–38] and previous investigations [17], the bands at 2208, 2179 and 2166 cm^{-1} are assigned to three kinds of Ti^{4+}–CO species formed with Ti^{4+} cations of different acidities (α, β and γ, respectively). The band at 2127 cm^{-1} is due to the ^{13}CO satellite of the 2179 cm^{-1} band. The band at 2107 cm^{-1} characterizes Au^0–CO species [10–13, 15, 16, 22].

Evacuation of the sample at 100 K and at increasing temperatures (up to ambient one) leads to gradual disappearance of the carbonyls of Ti^{4+} cations (Fig. 2, spectra b–k). As already reported [36–38], the band at 2179 cm^{-1} is shifted to 2190 cm^{-1} when the CO coverage decreases. The Au^0–CO band at 2107 cm^{-1} also decreases in intensity and is remarkably blue shifted, up to 2128 cm^{-1}, during evacuation (Fig. 2, spectrum k). With a lower coverage, a very weak band at 2138 cm^{-1} becomes observable and is the most resistant one towards evacuation (Fig. 2, spectrum k). However, this band, assigned to $Au^{\delta+}$–CO species [13–16, 20, 24, 27], also disappears after evacuation at temperatures higher than 100 K (spectra not shown).

In summary, the experiment demonstrates that, although a very small fraction of oxidized gold sites remains on the surface, gold is mostly in the form of a metal on the sample evacuated at 673 K.

Low-temperature CO adsorption on 4 wt.% Au/TiO_2 heated in oxygen at 373 K

The sample was heated in oxygen (4.7 kPa) at 373 K for 1 h and then evacuated for 15 min at 473, 573 and 673 K.

Low-temperature CO adsorption on the sample evacuated at 573 K results in the appearance of the

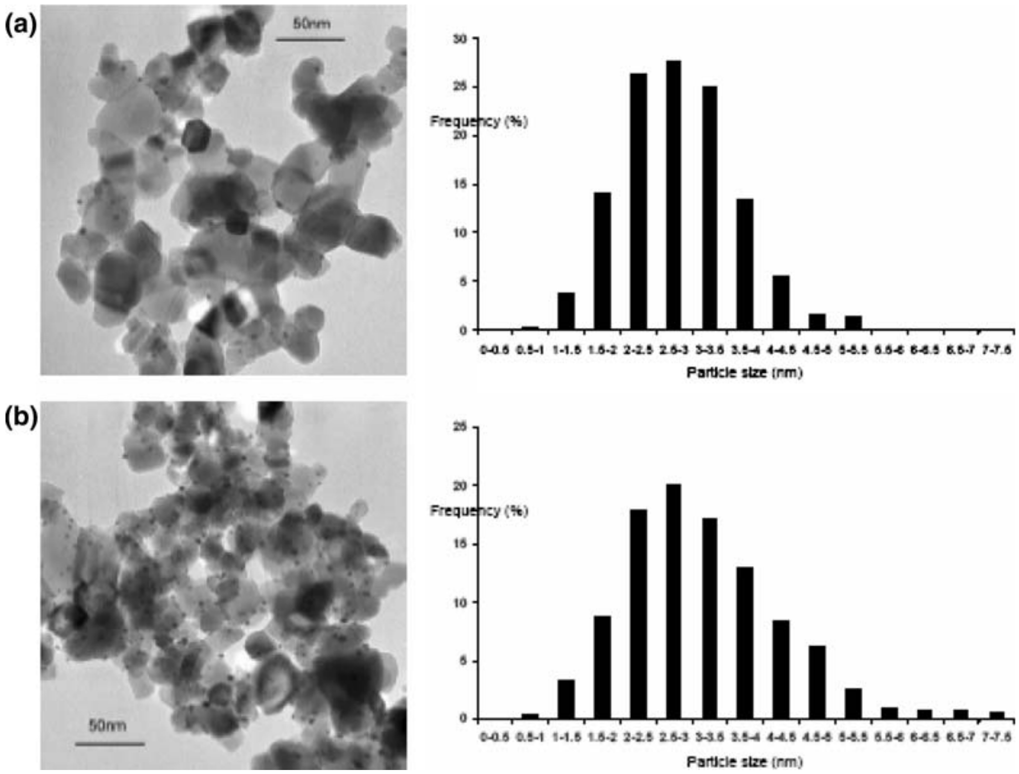

Fig. 1 TEM pictures and particle size distribution of the 0.7 wt.% Au/TiO$_2$ (**a**) and 4 wt.% Au/TiO$_2$ (**b**) catalysts calcined at 673 K

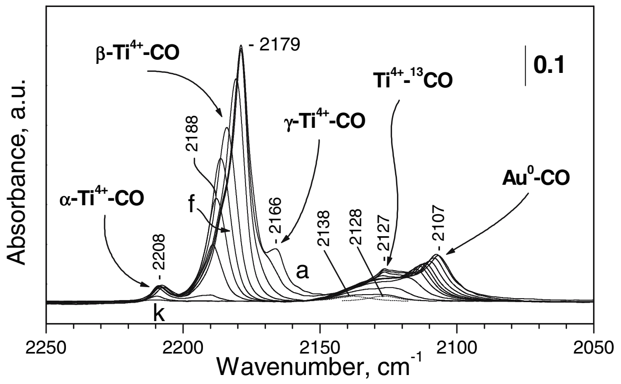

Fig. 2 FTIR spectra of CO adsorbed on the 4 wt.% Au/TiO$_2$ sample evacuated at 673 K. Adsorption of 400 Pa CO at 100 K, followed by evacuation at 100 K (**a**–**e**) and increasing temperatures up to ambient (**f**–**k**)

already described bands due to Ti^{4+}–^{12}CO (2208, 2179 and 2166 cm^{-1}, not shown) and Ti^{4+}–^{13}CO (2127 cm^{-1}) species (Fig. 3, spectrum a). In addition, a Au$^{\delta+}$–CO band at 2140 cm^{-1} [13–16, 20, 24, 27] and a weak Au^0–CO band at 2107 cm^{-1} [6, 10–19, 22, 25, 26, 28–33] have been registered (Fig. 3, spectrum a). The band at 2140 cm^{-1} is most resistant towards evacuation, but disappears from the spectrum at temperatures around the ambient (Fig. 3, spectra b–h). It has also been found that the band is coverage independent. The band at 2107 cm^{-1} decreases in intensity during evacuation and is simultaneously blue shifted, as typical of Au^0–CO species. Separate experiments have demonstrated (spectra not shown) that when the sample is evacuated at 473 K, the only deteclable gold carbonyls are those at 2140 cm^{-1}. These results demonstrate that interaction of the sample with oxygen leads to conversion of all Au^0 sites able to adsorb CO into Au$^{\delta+}$ sites. However, during evacuation at 573 K a small fraction of the Au$^{\delta+}$ sites are reduced again to Au^0, i.e. the oxidation-reduction is a reversible process.

The sample was then evacuated at 673 K. The spectra registered after subsequent low-temperature CO adsorption were similar to the spectra obtained with the sample initially evacuated at 673 K (compare Figs. 2 and 4). This implied that reduction of Au$^{\delta+}$ to Au^0 had occurred. Only the relative intensity of the Au$^{\delta+}$–CO band was somewhat higher probably because of the shorter evacuation time (15 min instead of 1 h).

In summary, the results show that:

- Calcination of the sample at 673 K followed by evacuation at the same temperature leads to full reduction of gold.
- Subsequent interaction of the sample with oxygen at 373 K leads to oxidation of surface metallic gold sites to Au$^{\delta+}$ sites.

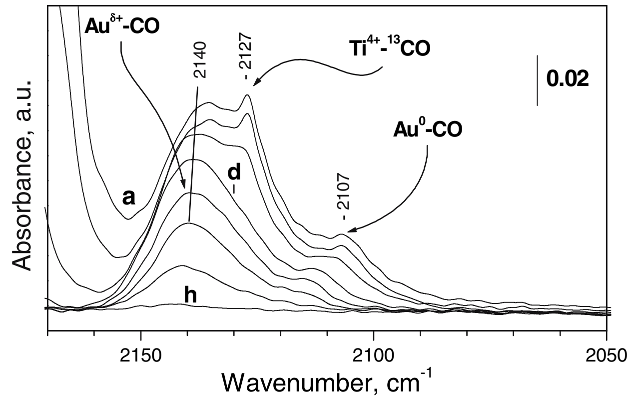

Fig. 3 FTIR spectra of CO adsorbed on the 4 wt.% Au/TiO_2 sample heated in oxygen at 373 K and evacuated at 573 K. Adsorption of CO (400 Pa equilibrium pressure) at 100 K, followed by evacuation at 100 K (**a**–**c**) and at increasing temperatures up to ambient (**d**–**h**)

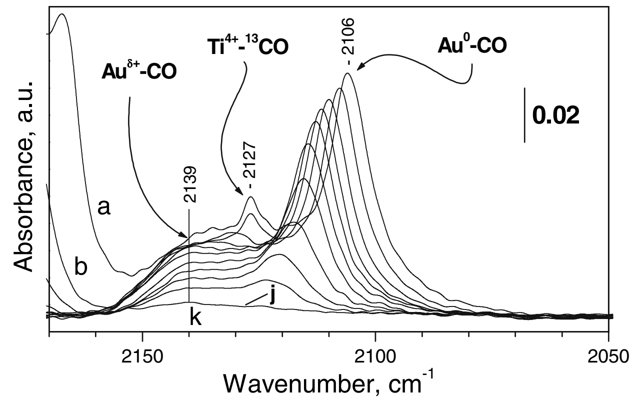

Fig. 4 FTIR spectra of CO adsorbed on the 4 wt.% Au/TiO_2 sample heated in oxygen at 373 K and evacuated at 673 K. Adsorption of CO (400 Pa equilibrium pressure) at 100 K, followed by evacuation at 100 K (**a**, **b**) and at increasing temperatures up to ambient (**c**–**k**)

- The Au$^{\delta+}$ sites are stable up to ca. 573 K. However, during evacuation at 573 K they start to be reduced to Au^{0} sites and this process is almost complete at 673 K.

Experiments were also performed with a sample heated in oxygen at 673 K and then evacuated for 15 min at 523 K. We had already established that this evacuation temperature was too low to reduce the Au$^{\delta+}$ sites. Indeed, no metallic gold was detected by subsequent low temperature CO adsorption on the sample. We detected an Au$^{\delta+}$–CO band that appeared at 2137 cm^{-1}, almost at the same frequency as for the sample oxidized at 373 K. These results indicate that the interaction of the sample with oxygen at 673 K also led to oxidation of surface metal gold atoms. They also demonstrated that the temperature of interaction of gold particles with oxygen (373–673 K) did not affect the nature of the oxidized sites.

Low-temperature CO adsorption on 4 wt.% Au/TiO_2 heated in a NO + O_2 mixture

We have recently reported that oxidation of gold is more effective when a NO + O_2 mixture is used as oxidizing media instead of oxygen [16]. The sample was treated for 30 min in the presence of NO (1 kPa) and O_2 (2 kPa) at 673 K and then evacuated for 30 min at 573 K. It is well known that heating oxide samples in a NO + O_2 mixture results in formation of nitrates [39]. However, these species have almost completely decomposed during the evacuation of our sample at 573 K (spectra not shown).

Subsequent low-temperature CO adsorption on the sample leads to the appearance (in addition to the carbonyls of titanium cations) of a band at 2157 cm^{-1}, which slightly shifts to 2154 cm^{-1} during evacuation (Fig. 5). This band is resistant towards evacuation at 100 K but disappears at room temperature. Note that after reaching 2154 cm^{-1} the band becomes coverage independent.

The band at 2154 cm^{-1} is situated at a much higher frequency than the bands already assigned to Au$^{\delta+}$–CO species and observed with the sample heated in oxygen. However, its frequency is lower than that of the bands reported for Au^{+}–CO species (2175–2160 cm^{-1}). Therefore, the band at 2154 cm^{-1} can be assigned to Au$^{\delta'+}$–CO complexes with $\delta' > \delta$.

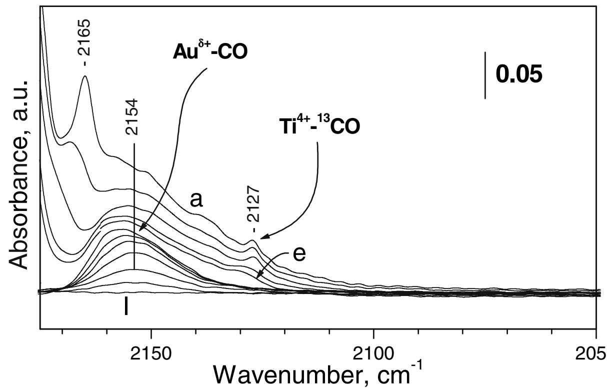

Fig. 5 FTIR spectra of CO adsorbed on the 4 wt.% Au/TiO_2 sample heated in a NO + O_2 mixture at 673 K and evacuated at 573 K. Adsorption of CO (400 Pa equilibrium pressure) at 100 K, followed by evacuation at 100 K (**a**–**e**) and increasing temperatures up to ambient (**f**–**l**)

Low-temperature CO adsorption on 0.7 wt.% Au/TiO_2 heated in a NO + O_2 mixture

The results obtained with the sample containing 0.7 wt.% Au will be only briefly described. Initially the sample was heated in a NO + O_2 mixture at 573 K and evacuated at the same temperature. Then CO was adsorbed on the sample at 100 K. In addition to the carbonyls formed with the support, a band at 2176 cm^{-1} was detected. The same band was observed when the oxidation was performed at higher temperatures (see Fig. 6). The band at 2176 cm^{-1} was resistant towards evacuation and was assigned to Au^+–CO species formed with "isolated" Au^+ cations. Hence, the results demonstrate an easier oxidation of metallic gold with the 0.7 wt.% Au sample than with the sample containing 4 wt.%.

Discussion

As already mentioned, the present work is focused, to a big extent, on the nature of the $Au^{\delta+}$ sites. Before starting the discussion, it is important to recall the following observations made by various authors:

- Heating of Au^{n+}/TiO_2 samples at T > 673 K, even in the presence of oxygen, leads to formation of metallic gold particles [10–13, 22].
- Not all gold atoms from the surface of the metal gold particles are able to adsorb CO. CO adsorption occurs on low-coordinated sites only [11, 15, 16, 18, 19, 22].
- Oxidation of gold particles occurs, to some extent, in the presence of oxygen [3, 12, 17, 25, 29, 32].

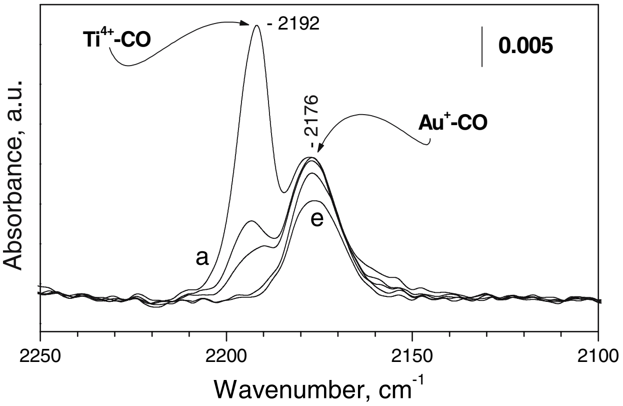

Fig. 6 CO adsorption on the 0.7 wt.% Au/TiO_2 sample heated in a NO + O_2 mixture at 673 K. Adsorption of CO (400 Pa equilibrium pressure) at 100 K, followed by evacuation at 100 K (**a**, **b**) and at increasing temperatures up to ambient (**c**–**e**)

Our TEM results confirm the formation of gold nanoparticles (<5 nm) after calcination at 673 K. The IR spectra of CO adsorbed on the 4 wt.% sample evacuated at 673 K, revealed that the gold sites able to form carbonyls were mostly metallic. We shall denote further on these "active" sites as Au^0_{act}, in contrast to gold sites on the surface of the particles that do not absorb CO (Au^0_{inert}) (See Scheme 1a).

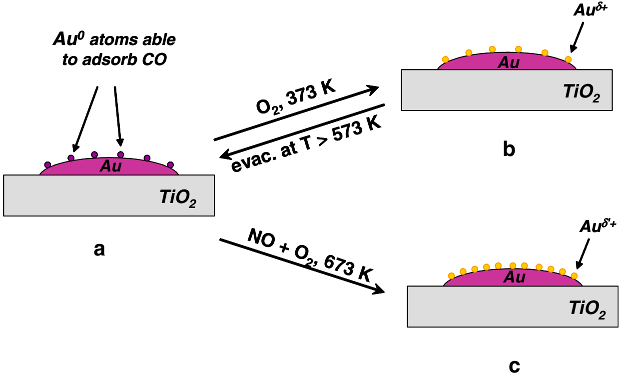

Scheme 1

Interaction of the sample with oxygen at 373 K, transforms the Au^0_{act} sites into $Au^{\delta+}$ sites. This process is reversible, since subsequent evacuation at T > 573 K leads to reduction of the $Au^{\delta+}$ sites to Au^0. It is interesting to estimate the concentration of both kinds of sites but it is difficult to make precise calculations of the number of sites on the basis of the intensities of the IR carbonyl bands because of the difference in their extinction coefficients. However, the extinction coefficients of the carbonyl bands of Au^0–CO and $Au^{\delta+}$–CO species should not differ drastically, because the π-back donation is expected to be similar. Note that the extinction coefficient of the carbonyl bands hardly depends on the formation of electrostatic and σ-bonds but is strongly enhanced by the π-bonding [7]. Inspection of the results shows that the intensity of the $Au^{\delta+}$–CO bands registered with the sample oxidized with oxygen (Fig. 7, spectrum a), is similar to that of the Au^0–CO band obtained with the sample evacuated at 673 K (Fig. 7, spectrum b). These results indicate that the number of the Au^0_{act} and $Au^{\delta+}$ sites is almost the same. The reversible interconversion between the $Au^{\delta+}$ and Au^0_{act} sites is presented on Scheme 1.

Oxidation of a gold atom normally results in electron transfer from gold to oxygen and formation of gold cations. Probing the $Au^{\delta+}$ sites with CO suggests that their charge is between 0 and 1+. Therefore we can propose the following model: oxidation of Au^0_{act} leads to formation of Au^+ cations located on the surface of the gold metal particles. In this way electron transfer from the gold particle to the cations can occur, thus decreasing their effective charge. This hypothesis

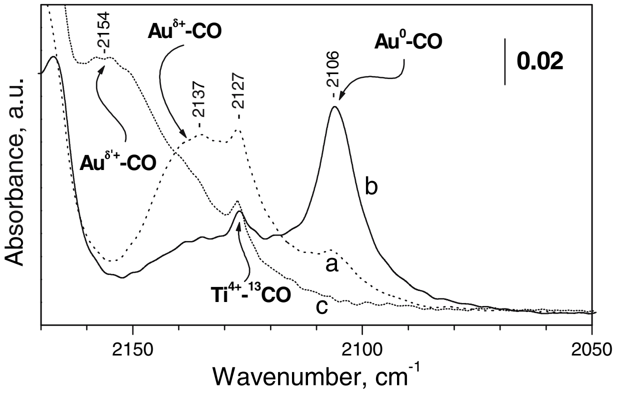

Fig. 7 Selected spectra from Fig. 4 (sample oxidized by O_2 and evacuated at 573 K) (**a**), Fig. 5 (sample oxidized by O_2 and evacuated at 673 K) (**b**) and Fig. 6 (sample oxidized by NO + O_2) (**c**)

explains the frequency and the stability of the $Au^{\delta+}$–CO species that are intermediate between those typical of Au^+–CO and Au^0–CO species.

Recent studies of some of us [34, 40], using X-ray absorption spectroscopies (EXAFS and XANES), showed supported gold particles smaller than 3 nm to be reactive to air, at least between room temperature and 500 K. This was attested by the presence of oxygen atoms in the coordination shell of gold: up to 15% of the atoms of the gold particles were oxidized [34, 40]. The same studies showed that larger particles, i.e. exposing a higher number of sites of flat surfaces, were not oxidized, which is in agreement with the fact that gold foil is unable to adsorb or dissociate oxygen [41, 42]. Other examples of partial oxidation of metallic gold particles have been reported for Au/TiO_2 and Au/Al_2O_3 after calcination at 623 K and exposure to air at room temperature, and even complete oxidation for Au/MgO exposed to O_2 at high temperature [43, 44]. All these cases concern mainly small gold nanoparticles (<5 nm). XANES studies have also revealed that the oxidized gold formed after exposure to oxygen is readily reduced in the co-presence of CO and O_2 at room temperature [40], this indicating that the reoxidation is reversible.

It was also found that the oxidation of gold with a NO + O_2 mixture was more efficient than oxidation with oxygen only. The effective charge of the $Au^{\delta'+}$ sites formed in this way was higher than that of the $Au^{\delta+}$ sites: the frequency of the respective carbonyl band (2154 cm^{-1}) was closer to those of bands typical of carbonyls of isolated Au^+ cations (2175–2160 cm^{-1}). Note that the intensity of the $Au^{\delta'+}$–CO band (Fig. 7, spectrum c) was higher than that of the band due to $Au^{\delta+}$–CO species (Fig. 7, spectrum a). This suggested that not only the Au^0_{act} sites, but also some Au^0_{inert} surface sites had been oxidized to cations (Scheme 1c). Thus, the higher frequency of the $Au^{\delta'+}$–CO species can be explained as follows: because of the larger number of cationic sites on the surface of each gold particle, they compete for electrons from the metal particle and the transfer is not so effective. As a result, the surface $Au^{\delta'+}$ sites appear more positively charged.

The results also demonstrate that the nature of the oxidized gold species obtained when the oxidation is carried out with a NO + O_2 mixture differs for the two samples. This is most probably related to the gold particle size. With the 0.7 wt.% sample, whose average gold particle size is 3.2 nm, the oxidation is more efficient and leads to formation of ''isolated'' gold cations, i.e. cations not interacting directly with metal particles. With the 4.0 wt.% Au sample (average particle size 3.9 nm) $Au^{\delta'+}$ sites located on the metal surface are formed.

Conclusions

Interaction of metal gold nanoparticles with oxygen leads to oxidation of part of the surface gold sites (those that are ''active'' in adsorption of CO) and the cations formed are characterized by a partial positive charge $\delta+$ ($0 < \delta < 1$) because of the transfer of electrons from gold particles. Evacuation at T > 573 K results in reduction of these sites to metallic sites.

Oxidation of metal gold particles is more effective when performed with a NO + O_2 mixture, than with oxygen. In this case a higher number of metal gold sites are oxidized and the cations formed are more positively charged. When the particles are small enough, ''isolated'' gold cations, i.e. cations not interacting directly with metal particles, are formed.

Acknowledgments The authors are grateful to Egide, France (Project ECO-NET No 101186SH). We also thank S. Pronier for the TEM analyses and L.T.N. Nguyen for the preparation of the Au/TiO_2 (0.7 Au wt %) sample.

References

1. Arii S, Mortin F, Renouprez AJ, Rousset JL (2004) J Am Chem Soc 126:1199
2. Haruta M (2002) CATTECH 6:102
3. Grunwaldt J-D, Maciejewski M, Becker O, Fabrizioli P, Baiker A (1999) J Catal 186:458
4. Boyd D, Golunski S, Hearne G, Magadzu T, Mallick K, Raphulu M, Venugopal A, Scurrell M (2005) Appl Catal A292:76
5. Fierro-Gonzalez JC, Gates BC (2004) J Phys Chem 108:16999

6. Minico S, Scire S, Crisafalli C, Visco A, Galvagno S (1997) Catal Lett 47:273
7. Hadjiivanov K, Vayssilov G (2002) Adv Catal 47:307
8. Davydov A (2003) Molecular Spectroscopy of Oxide Catalyst Surfaces. Wiley, Chichester
9. Knözinger H (1997) In: Ertl G, Knözinger H, Weitkamp J (eds), Handbook of Heterogeneous Catalysis, vol 2. Wiley–VCH, Weinheim, p 707
10. Boccuzzi F, Chiorino A, Tsubota S, Haruta M (1996) J Phys Chem 100:3625
11. Boccuzzi F, Chiorino A, Manzoli M (2000) Surf Sci 454–456:942
12. Boccuzzi F, Chiorino A, Manzoli M, Lu P, Akita T, Ichikawa S, Haruta M (2001) J Catal 202:256
13. Boccuzzi F, Chiorino A, Manzoli M (2002) Surf Sci 513:502–503
14. Guillemot D, Borovkov V, Kazansky V, Polisset-Thfoin M, Fraissard J (1997) J Chem Soc Faraday Trans 93:3587
15. Maciejewski M, Fabrizioli P, Grunwaldt J-D, Becker OS, Baiker A (2001) Phys Chem Chem Phys 3:3846
16. Venkov Tz, Fajerwerg K, Delannoy L, Klimev Hr, Hadjiivanov K, Louis C (2006) Appl Catal A301:106
17. Venkov Tz, Klimev Hr, Centeno MA, Odriozola JA, Hadjiivanov K (2006) Catal Commun 7:308
18. Jia J, Kondo JN, Domen K, Tamaru K (2001) J Phys Chem B 105:3017
19. Lemire C, Meyer R, Shaikhutdinov Sh, Freund H-J (2004) Surf Sci 552:27
20. Fierro-Gonzalez JC, Anderson BG, Ramesh K, Vinod CP, Niemantsverdriet JWH, Gates BC (2005) Catal Lett 101:265
21. Pestryakov A, Lunin V, Kharlanov A, Kochubey D, Bogdanchikova N, Stakheev A (2002) J Mol Struct 642:129
22. Boccuzzi F, Chiorino A, Manzoli M (2001) Mater Sci Eng C15:215
23. Carrettin S, Corma A, Iglesias M, Sanchez F (2005) Appl Catal A291:247
24. Gao Z-X, Sun Q, Chen H-Y, Wang X, Sachtler WMH (2001) Catal Lett 72:1
25. Yates DJC (1969) J Colloid Interface Sci 29:194
26. Okumura K, Yoshino K, Kato K, Niwa M (2005) J Phys Chem B109:12380
27. Grunwaldt JD, Baiker A (1999) J Phys Chem B103:1002
28. Haruta M (1997) Catal Surv Jpn 1:61
29. Boccuzzi F, Cerrato G, Pinna F, Strukul G (1998) J Phys Chem B 102:5733
30. Mihaylov M, Fierro-Gonzalez JC, Knozinger H, Gates B, Hadjiivanov K (2006) J Phys Chem B 110:7695
31. Concepción P, Carrettin S, Corma A (2006) Appl Catal A 307:42
32. Dekkers M, Lippits M, Nieuwenhuys B (1998) Catal Lett 56:195
33. Mohamed M, Salama T, Ichikawa M (2000) J Colloid Interface Sci 224:366
34. Miller JT, Kropf AJ, Zha Y, Regalbuto JR, Delannoy L, Louis C, Bus E, van Bokhoven JA (2006) J Catal 240:222
35. Zanella R, Giorgio S, Henry CR, Louis C (2002) J Phys Chem B 103:7634
36. Busca G, Saussey H, Saur O, Lavalley J-C, Lorenzelli V (1985) Appl Catal 14:245
37. Hadjiivanov K, Klissurski D (1996) Chem Soc Rev 25:61
38. Hadjiivanov K, Lamotte J, Lavalley J-C (1997) Langmuir 13:3374
39. Hadjiivanov K (2000) Catal Rev Sci Eng 42:71
40. van Bokhoven JA, Louis C, Miller JT, Tromp M, Safonova OV, Glatzel P, Ang Chemie, 2006, DOI: 10.1002/anie.200123456
41. Meyer R, Lemire C, Shaikhutdinov SK, Freund HJ (2004) Gold Bull 37:72
42. Richardson PC, Rossington DR (1971) J Catal 20:420
43. Fu L, Wu NQ, Yang JH, Qu F, Johnson DL, Kung MC, Kung HH, David VP (2005) J Phys Chem B 109:3704
44. Guzman J, Gates BC (2003) J Phys Chem B 107:2242